NATIONAL TRANSPORTATION SAFETY BOARD
Office of Research and Engineering
Vehicle Performance Division
Washington, D.C. 20594

December 13, 2017

Finite Element Modeling Study Report

A. ACCIDENT INFORMATION

Place	:	Graettinger, Iowa
Date	:	March 10, 2017
Vehicle	:	Union Pacific Ethanol Unit Train, UEGKOT-09
NTSB No.	:	DCA17MR007
Investigator	:	Michael Hiller

B. TOPICS ADDRESSED

Finite element (FE) modeling was used to examine the effects of rail profile and track support conditions on the deformation and stresses in 90-lb rail under tank car wheel loads.

C. DETAILS OF THE STUDY

Two 3-D finite element models of the 90-lb rail track were constructed. One model had a standard (unworn) rail profile and assumed stiff track support conditions. The other model had a worn rail profile based on measurements and assumed less stiff track support conditions. Stresses and rail deformations from the two models were compared. The FE modeling was carried out using the FE software Abaqus version R2016x.

1. Geometry

The geometry of the FE model is shown in Figure 1. The model consisted of a quarter of a track that was 565.5 inches long, which is approximately the length of a tank car. The model had symmetry planes in both the transverse plane (XY-plane in Figure 1) and the longitudinal plane (YZ-plane in Figure 1). Part of the rail was modeled in full 3-D and the rest of the rail was simplified as beam elements. The model also included simplified geometry of the crossties, the ballast and the subgrade. Some key dimensions of the model are summarized in Table 1. The wheels were included in the model for the purpose of applying loads to the rail. The wheels had 36-in diameters and their geometry was based on the AAR standard [Reference 1] with simplified straight flanges. The distance between the wheel centers was 70 inches, standard for 100-ton trucks.

Table 1. Key Model Dimensions

Dimension	Value (inch)
Crosstie half length	51
Crosstie width	9
Crosstie depth	7
Crosstie spacing	19.5
Ballast depth	24

Two rail profiles were modeled and are shown in Figure 2. The standard profile was based on drawings provided by Union Pacific [Reference 2]. The worn profile was derived from rail profile measurements using a MiniProf® rail profile measurement system. MiniProf® is a portable precision measurement tool designed for use in railroad environments and can be used during the on-scene phase of investigations. Wheel and rail profiles were independently captured with specialized measurement instruments that converted the measurement into an electronic format.

2. Material

The stiffness of the ballast and wooden crossties can vary, providing different levels of support for the track. Two sets of stiffness values, representing a “stiff” and a “soft” track support condition, were selected for this study. The values and their references are listed in Table 2. The ballast was modeled with a linear elastic-perfectly plastic material model, while the cross ties were modeled with a linear elastic material model.

Table 2. Material parameters for the crossties and the ballast

Material		Young’s Modulus (psi)	Poisson’s Ratio	Yield Stress (psi)	Reference
Crosstie	stiff	150,000	0.3	N/A	3
	soft	80,000	0.3	N/A	3
Ballast	stiff	60,000	0.3	120	4, 5
	soft	10,000	0.3	20	4, 5

The rail and wheels were made of steel and modeled with a linear elastic material model. The Young’s modulus of 29e6 psi and the Poisson’s ratio of 0.3, both typical of the material of steel, were used. The subgrade was modeled with a linear elastic material model with a Young’s modulus of 72,519 psi and Poisson’s ratio of 0.25, the same as in Reference 5.

3. Loads and Boundary Conditions

Symmetric boundary conditions were applied to the appropriate faces of the rail, crossties, ballast and subgrade, as shown in Figure 3. Please note that the symmetric

boundary condition for the rail was applied to the node of the beam representing the rail. Symmetric boundary conditions were also applied to the transverse face on the other end of the model (see Figure 4), making the model representative a continuous track and multiple cars in a periodic fashion. The bottom of the ballast was constrained for vertical displacements.

Both the ballast-subgrade and crosstie-ballast interfaces were modeled with Abaqus' mesh tie constraints. The 3-D portion of the rail was connected to the crossties also with tie constraints. For the portion of the rail modeled as beams, the beam nodes were connected to the corresponding areas on the crossties via coupling constraints (see Figure 5).

The wheel loads were applied by moving the wheels down through a specified displacement. Applying displacements to the wheels improved the convergence for the contact that develops between the wheels and the rail. The mounting surface of each wheel was constrained to a reference point located in the axle centerline via coupling constraints (see Figure 6). Only a downward displacement was allowed for the reference point. One wheel was positioned at the rail mid-span between two crossties (see Figure 1). The other wheel was positioned 70 inches away. The applied displacements for the two wheels were adjusted so that the applied wheel loads were approximately the same. The wheel load of interest was 50 kips per wheel, a magnitude that the rail could experience under dynamic conditions. A higher magnitude of 80 kips was also considered, which was toward the upper limit of wheel impact loads [Reference 6].

4. Mesh

The model was meshed with bi-linear brick solid elements (C3D8R in Abaqus) except for the portion of the rail modeled with beam elements, which was meshed with linear Timoshenko beam elements (B31 in Abaqus). To obtain the properties required to define the beam elements, the "meshed beam cross section" functionality in Abaqus was used. Specifically, the rail cross section was meshed with 2-D elements and a sub-model was created to compute the required properties including cross section centroid, shear center and stiffness properties. This was done for both the standard and the worn rail profiles. This approach ensured the portions of the rail modeled as 3-D solid and as beam elements to be equivalent from the structural mechanics point of view. To transition from the 3-D solid elements to the beam elements, coupling constraints were created linking the first beam element node to the solid element nodes on the transitioning surface (see Figure 7). Mesh statistics for the model are summarized in Table 3. The total number of degrees of freedom was 493,440 with the standard rail profile and 512,538 with the worn rail profile.

Table 3. Mesh statistics for the FE model

Part name	Element type	Number of elements	Typical mesh size (inch)
Rail, solid, standard profile	Solid	82,732	0.1, coarser away from contact point
Rail, solid, worn profile	Solid	77,774	0.1, coarser away from contact point
Rail, beam	Beam	42	4
Wheels (both)	Solid	18,816	0.2, coarser away from contact point
Crossties (all)	Solid	8,176	1.8
Ballast	Solid	28,116	2
Subgrade	Solid	2,520	8

5. Output

As previously discussed, two cases representing different track conditions were studied. The first case had the worn rail profile and used properties of soft crossties and ballast. This case was designed to simulate a deteriorated track condition and was the focus of the study. The second case had the standard rail profile and used properties of stiff crossties and ballast. This case was designed to simulate a good track condition and was used for comparison purposes.

Figure 8 shows vertical displacement contours for the case with a worn rail profile and soft track support. The wheel load was approximately 51 kips at the mid-span wheel and 52 kips at the other wheel. Figure 9 shows the deformed track with vertical displacement contours and the deformation magnified by 30 times. Figure 10 shows the longitudinal view of the deformed rail with the vertical displacement contours. The rail model was mirrored with respect to the tank car centerline to show the deformed rail over the length of the tank car. The deformation was also magnified 30 times. The peak rail deflection was 0.09 inches at the mid-span location where the wheel load was applied. For comparison, figure 11 shows the vertical displacement contour for the case with standard rail profile and stiff track support. Like the first case, the wheel load was approximately 51 kips at the mid-span wheel and 53 kips at the other wheel. Figure 12 compares the vertical displacement contours for the 3-D solid portion of the rail for the two cases. The peak rail deflection was 0.04 inches for the second case with a standard rail profile and stiff track support.

Figure 13 compares the Mises stress contours for the 3-D solid portion of the rail for the two cases. The upper limit of the plot legend was chosen to be 50 ksi. The peak stress occurred at the wheel-rail contact spots. Please note that the contact spots differed slightly between the two cases. This was due to the difference in rail profiles. Figure 14 compares the longitudinal stress (Szz) contours between the two cases. The plot contour values were chosen to highlight stresses in the range from -20 ksi to +20 ksi. The rail in the case with a worn rail profile and soft track support showed higher tensile longitudinal

stresses due to the more pronounced bending deformation it experienced. The peak tensile longitudinal stresses occurred at the bottom of the rail where the wheel forces were applied, as well as at the top of the rail in the mid-point of where the wheel forces were applied. Figures 15 and 16 compare the transverse stress (Sxx) contours between the two cases at the rail cross sections where the wheel loads were applied. The plot contour values were chosen to highlight stresses in the range from -10 ksi to +10 ksi. The case with a worn rail profile and soft track support showed higher tensile transverse stresses in the middle of the rail head. This was because the worn rail profile had a smaller rail head area.

Figure 17 shows the vertical displacement contours for the case with a worn rail profile and soft track support at higher wheel loads. The wheel load was approximately 80 kips at both wheels. Figure 18 shows the longitudinal view of the deformed rail with the vertical displacement contour. The rail model was mirrored with respect to the tank car centerline and the deformation was magnified 30 times. The peak rail deflection was 0.16 inches at the mid-span location where the wheel load was applied. For comparison, figure 19 shows the vertical displacement contours for the case with standard rail profile and stiff track support. The wheel load was approximately 80 kips at the mid-span wheel and 83 kips at the other wheel. Figure 20 compares the vertical displacement contours for the 3-D solid portion of the rail for the two cases. The peak rail deflection was 0.06 inches for the second case with standard rail profile and stiff track support.

D. REFERENCES

1. Manual of Standard and Recommended Practices, Wheels and Axles Manual, Association of American Railroads, 2011.
2. 90-lb Rail Sections, Union Pacific Railroad Engineering Standards, 1998.
3. Recycled Plastic Railway Ties, Analysis and Comparison of Sleeper Parameters and the Influence on Track Stiffness and Performance, Aran van Belkom, Railway Engineering 2015.
4. Report on CSX Derailment on Metro-North Tracks in Bronx, NY, July 18, 2013, the Volpe National Transportation Systems Center, 2014.
5. Failure Analysis of Railroad Concrete Crossties in the Center Negative Flexural Mode using Finite Element Method, Hailiang Yu, Brian P. Marquis and David Y. Jeong, Journal of Rail and Rapid Transit, 231(5), pp 610-619, 2017.
6. Mechanical Inspections and Wheel Impact Load Detector Standards for Trains Transporting Large Amounts of Class 3 Flammable Liquids, Safety Advisory 2015-01, Federal Railroad Administration, 2015.

Xiaohu Liu
Finite Element Analyst

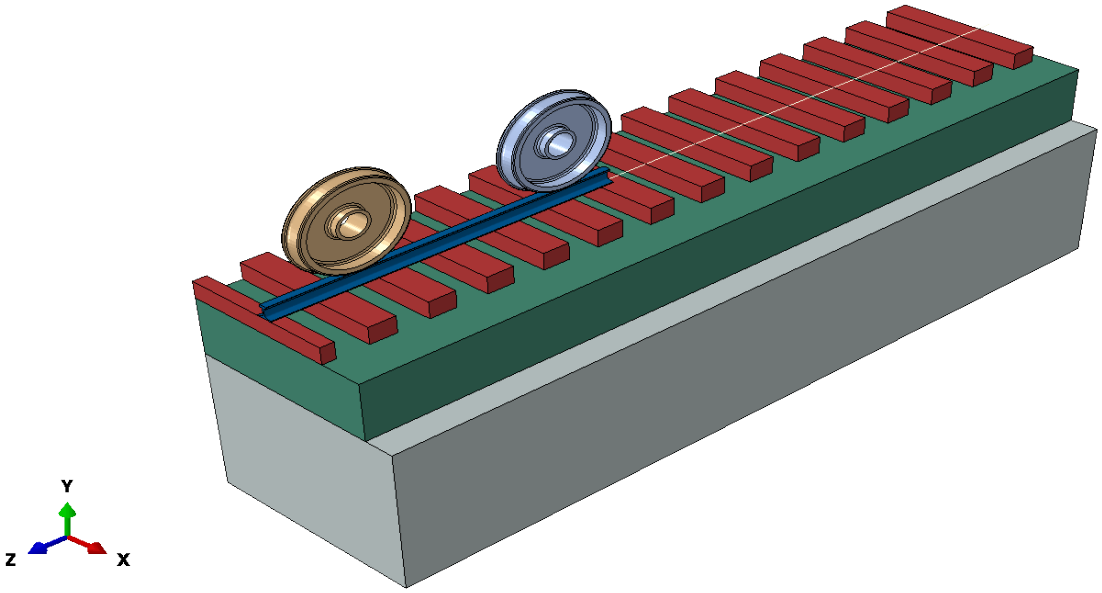

Figure 1. Geometry of the track model.

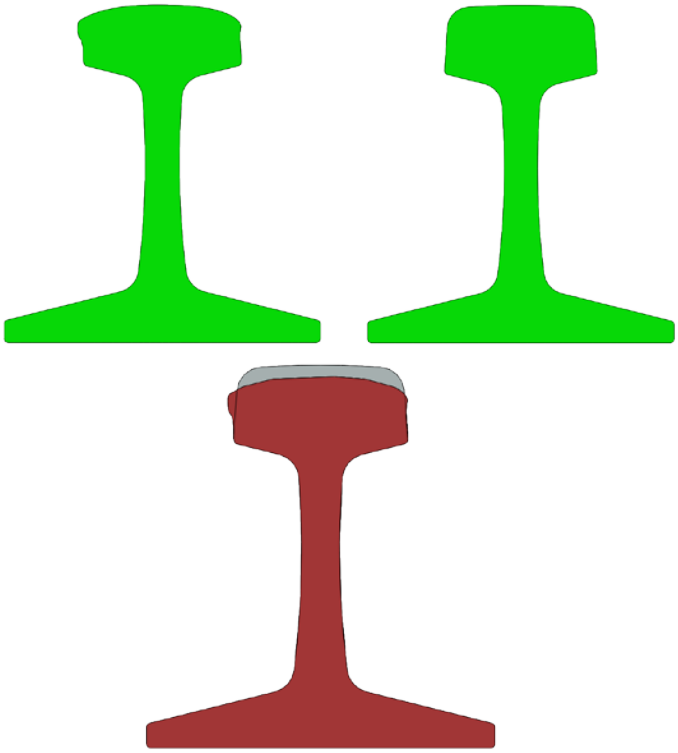

Figure 2. The two rail profiles considered: worn (top left), standard (top right) and their comparison (bottom).

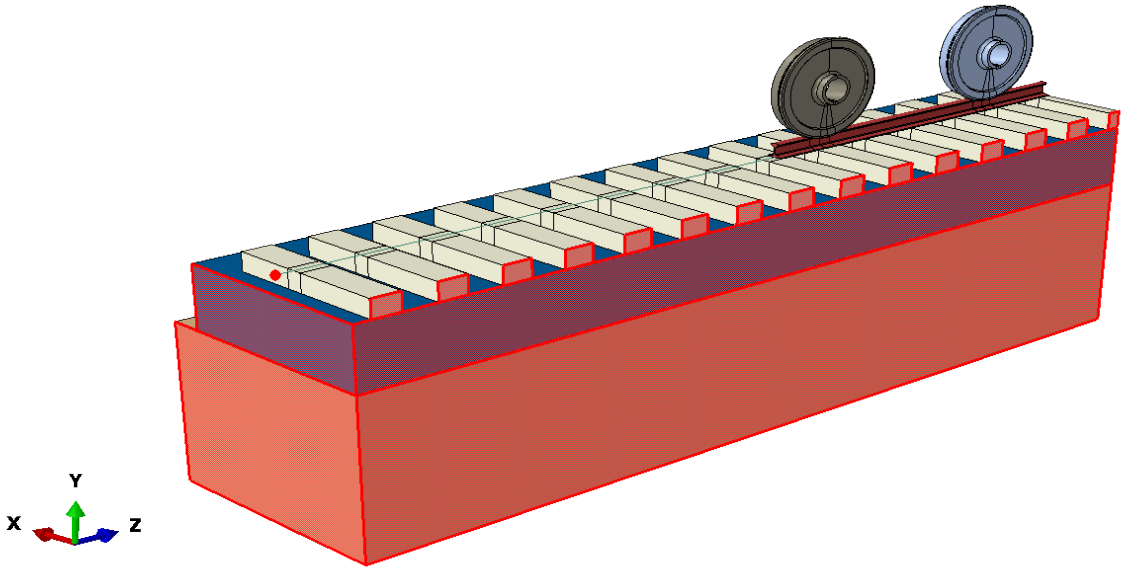

Figure 3. Faces (highlighted in red) with symmetric boundary conditions.

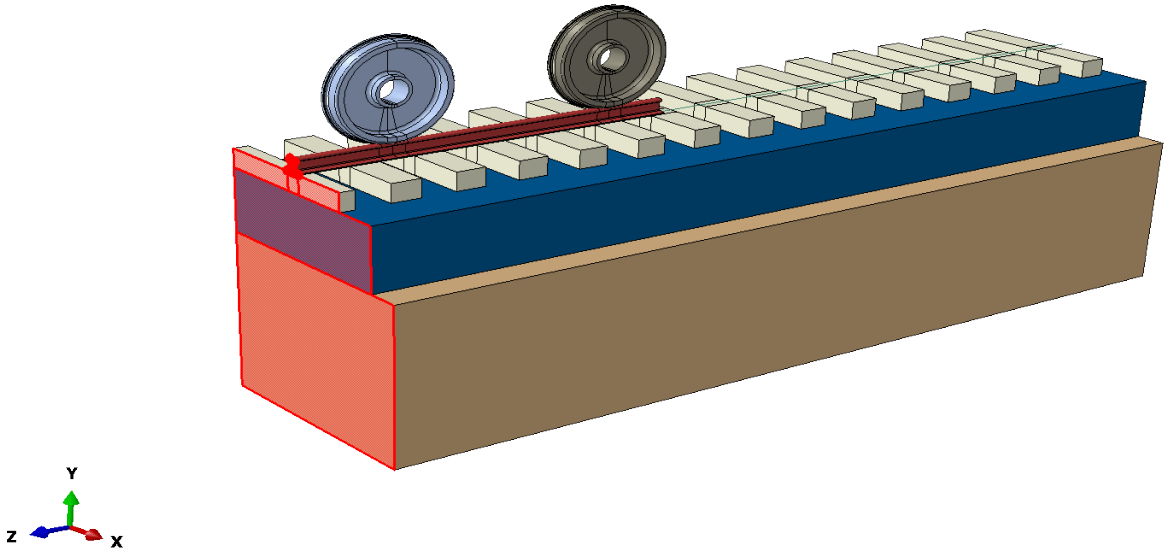

Figure 4. Faces (highlighted in red) with additional symmetric boundary conditions.

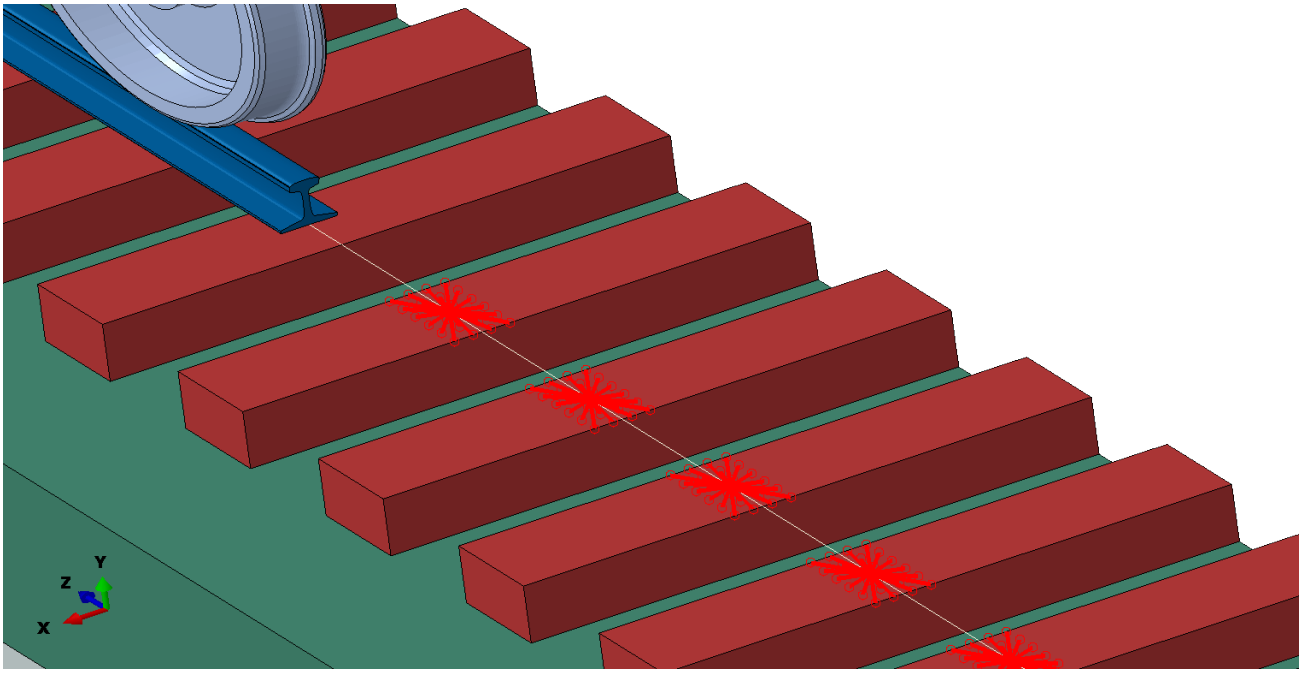

Figure 5. Coupling constraints (shown in red lines) between the beam portion of the rail and the crossties.

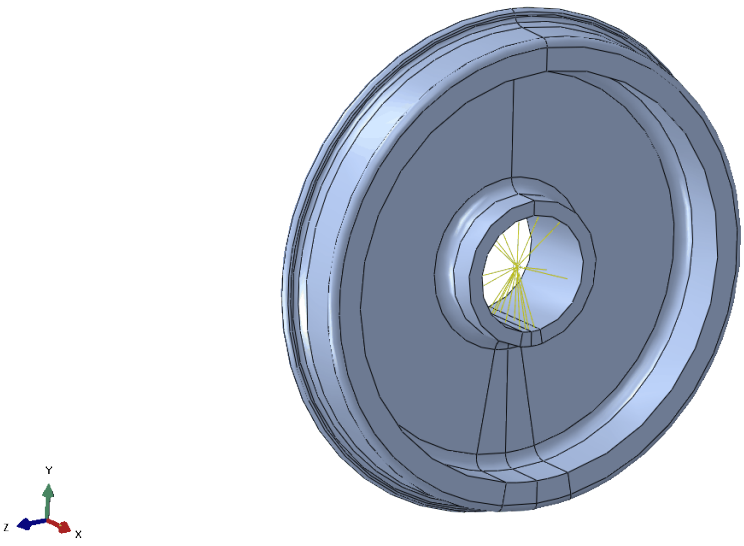

Figure 6. Coupling constrains (shown in yellow lines) between the wheel reference point and the wheel mounting surface.

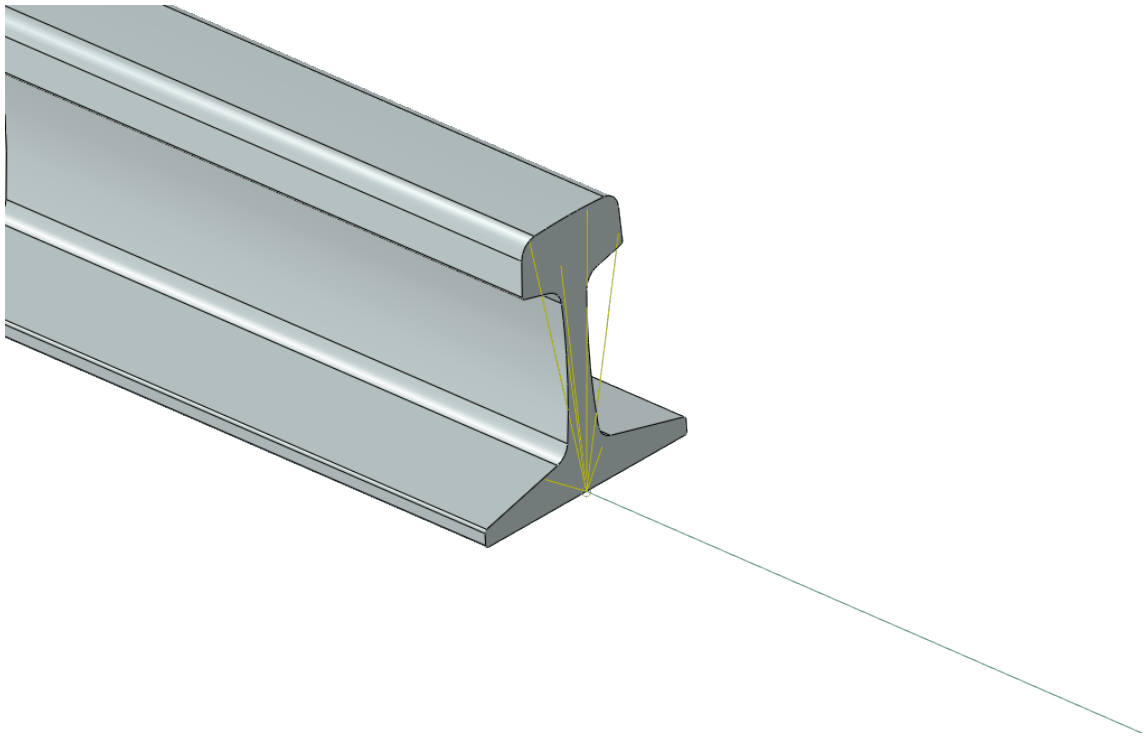

Figure 7. Coupling constraints (shown in yellow lines) connecting the beam node and the 3D solid face of the rail.

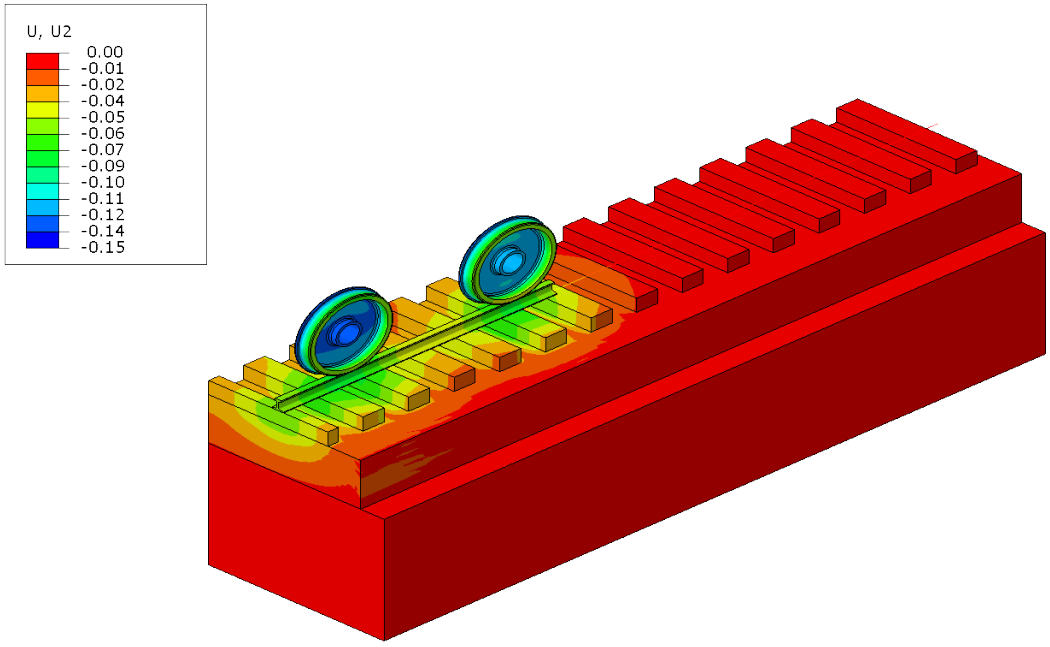

Figure 8. Vertical displacement (unit: inches) contour, the entire model, the case with worn rail profile and soft track support.

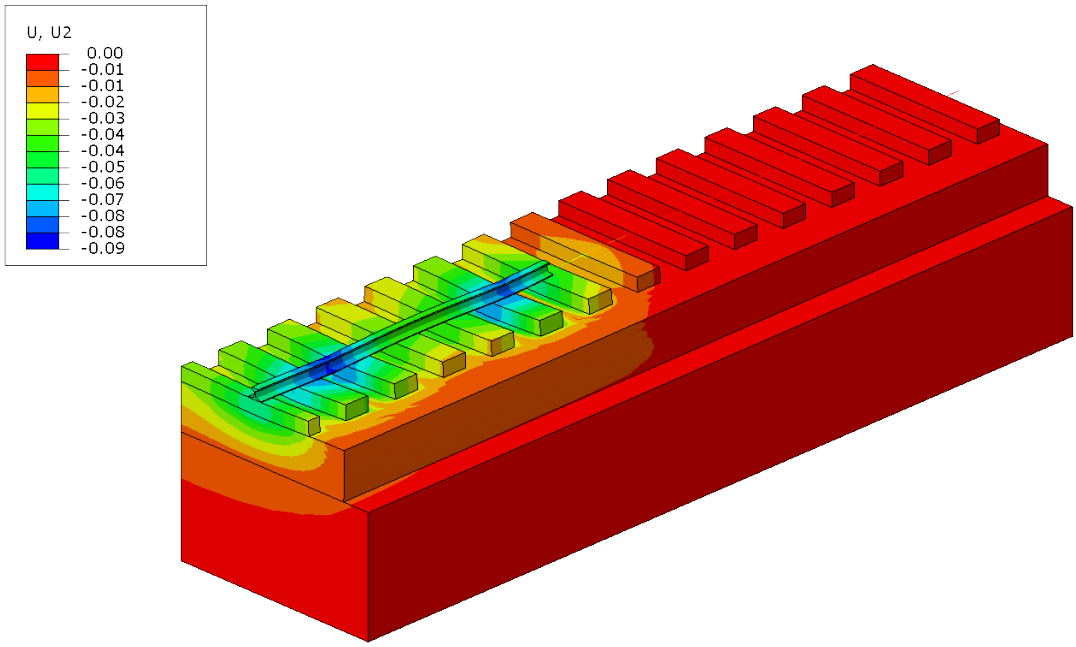

Figure 9. Vertical displacement (unit: inches) contour, the track structure, the case with worn rail profile and soft track support, deformation magnified 30 times.

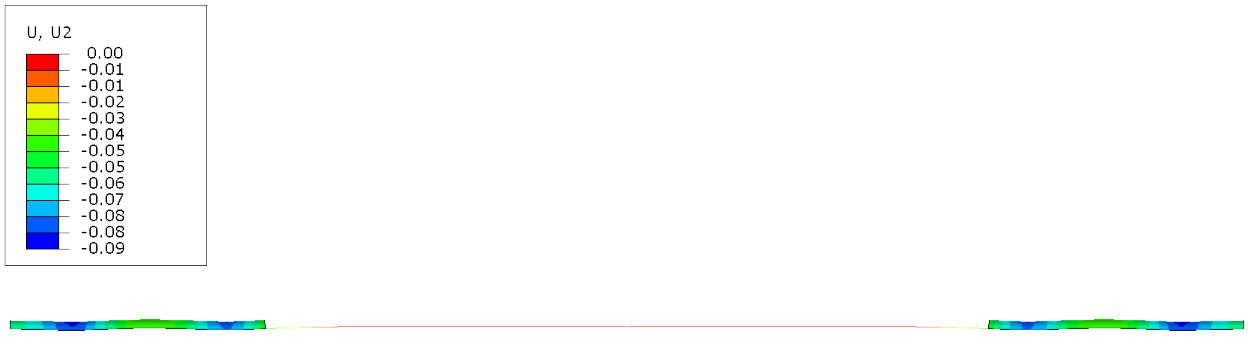

Figure 10. Vertical displacement (unit: inches) contour, the rail, the case with worn rail profile and soft track support, deformation magnified 30 times, structure mirrored with respect to the tank car center line.

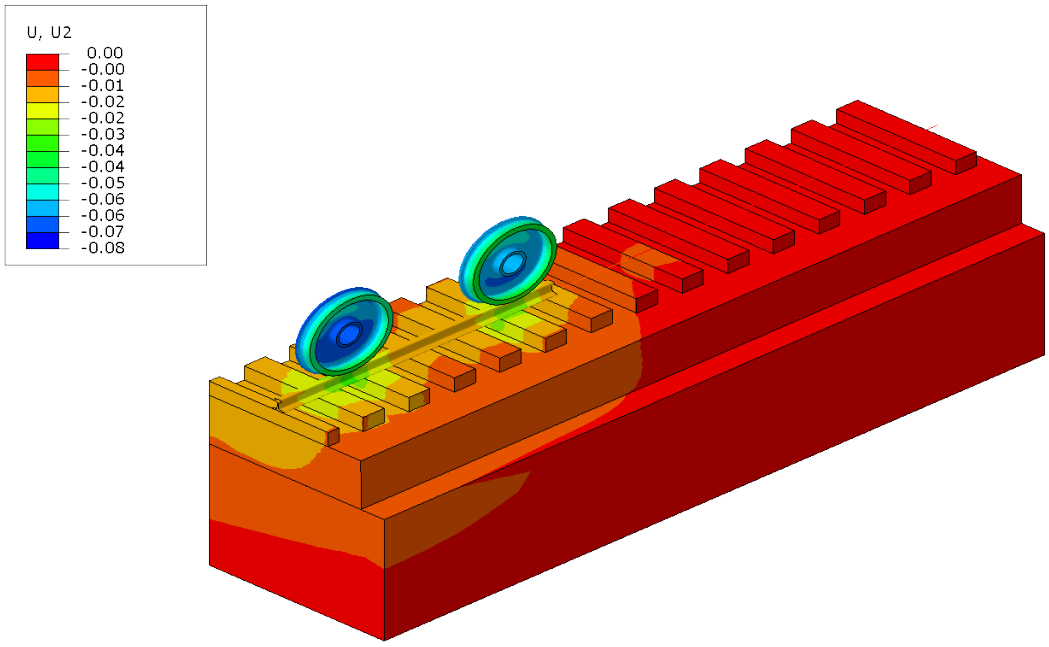

Figure 11. Vertical displacement (unit: inches) contour, the entire model, the case with standard rail profile and stiff track support.

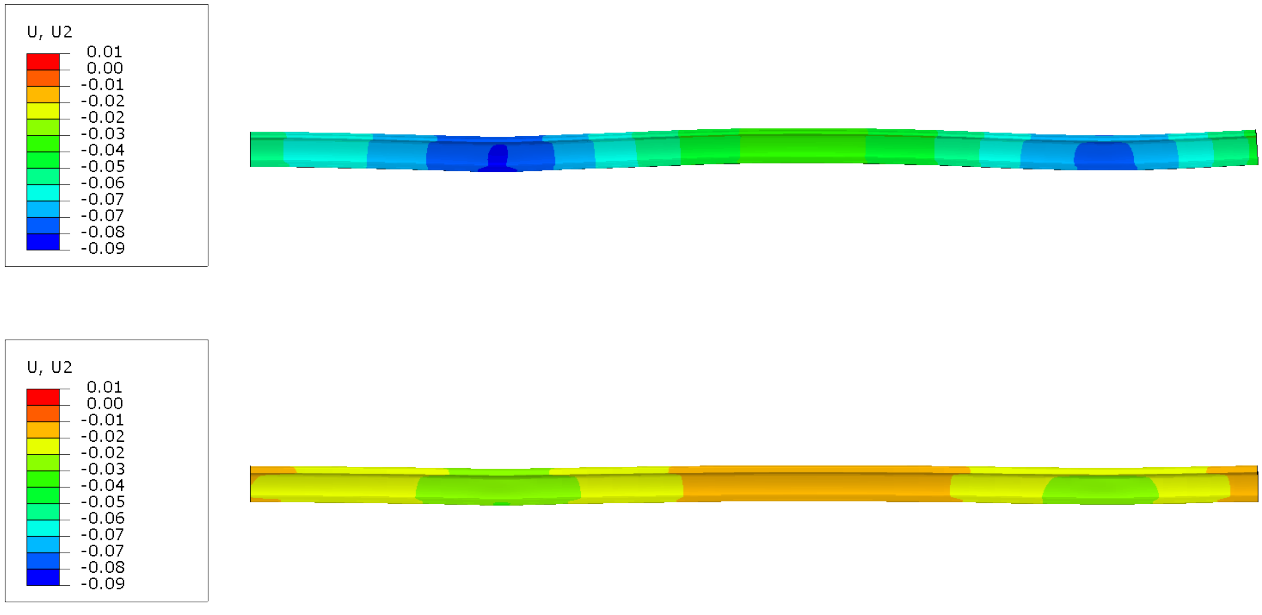

Figure 12. Comparison of the vertical displacement contours on the rail between the two cases, deformation magnified 30 times: worn rail profile with soft track support (top) and standard rail profile with stiff track support (bottom).

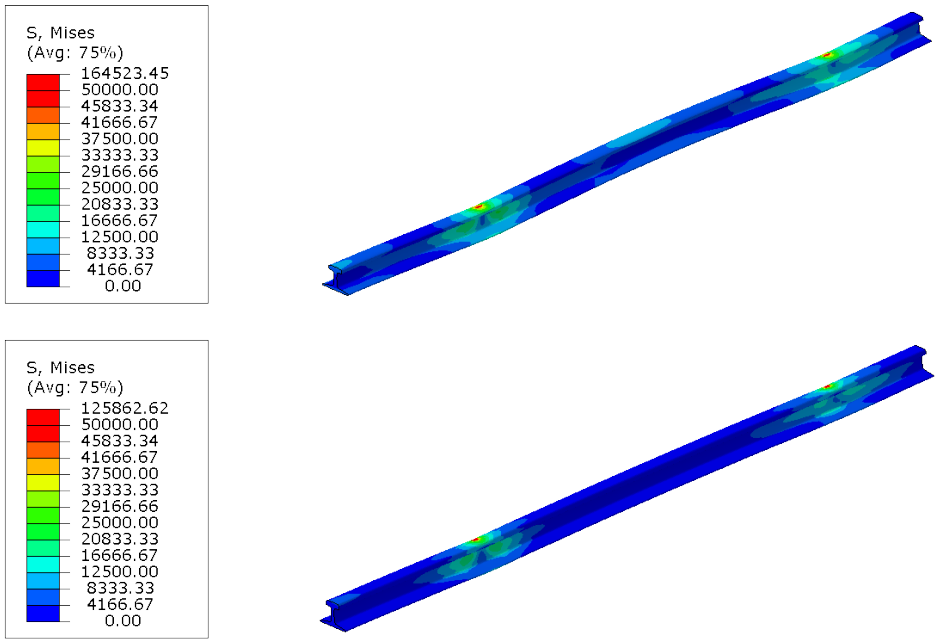

Figure 13. Comparison of the Mises stress (unit: psi) contours on the rail between the two cases, deformation magnified 30 times: worn rail profile with soft track support (top) and standard rail profile with stiff track support (bottom).

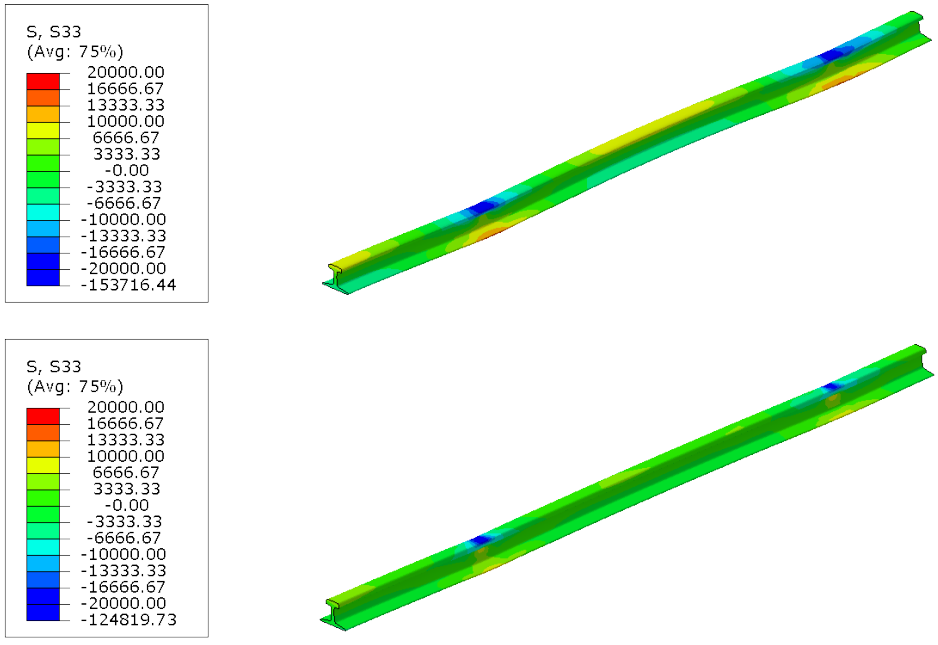

Figure 14. Comparison of the longitudinal stress (Szz, unit: psi) contours on the rail between the two cases, deformation magnified 30 times: worn rail profile with soft track support (top) and standard rail profile with stiff track support (bottom).

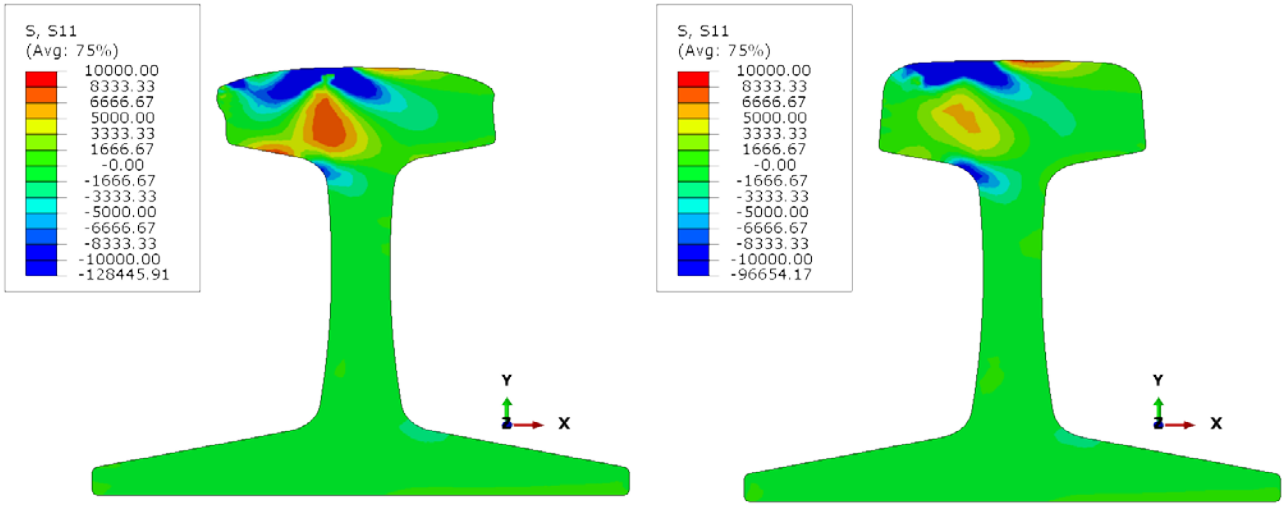

Figure 15. Comparison of the transverse stress (Sxx, unit: psi) contours on the rail cross section at the mid-span wheel load location: worn rail profile with soft track support (left) and standard rail profile with stiff track support (right).

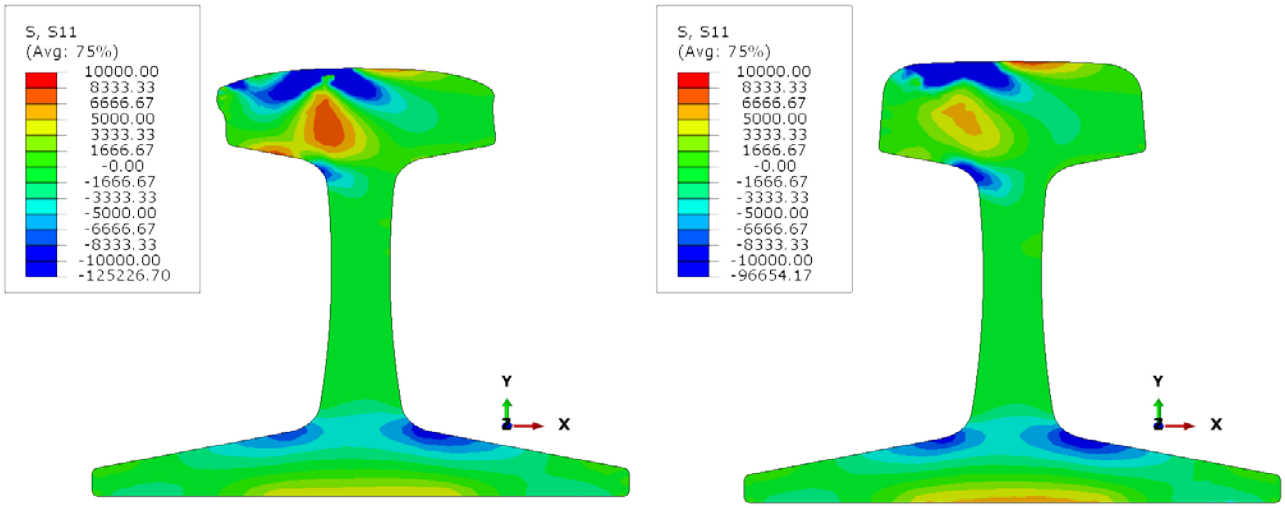

Figure 16. Comparison of the transverse stress (Sxx, unit: psi) contours on the rail cross section at the second wheel load location: worn rail profile with soft track support (left) and standard rail profile with stiff track support (right).

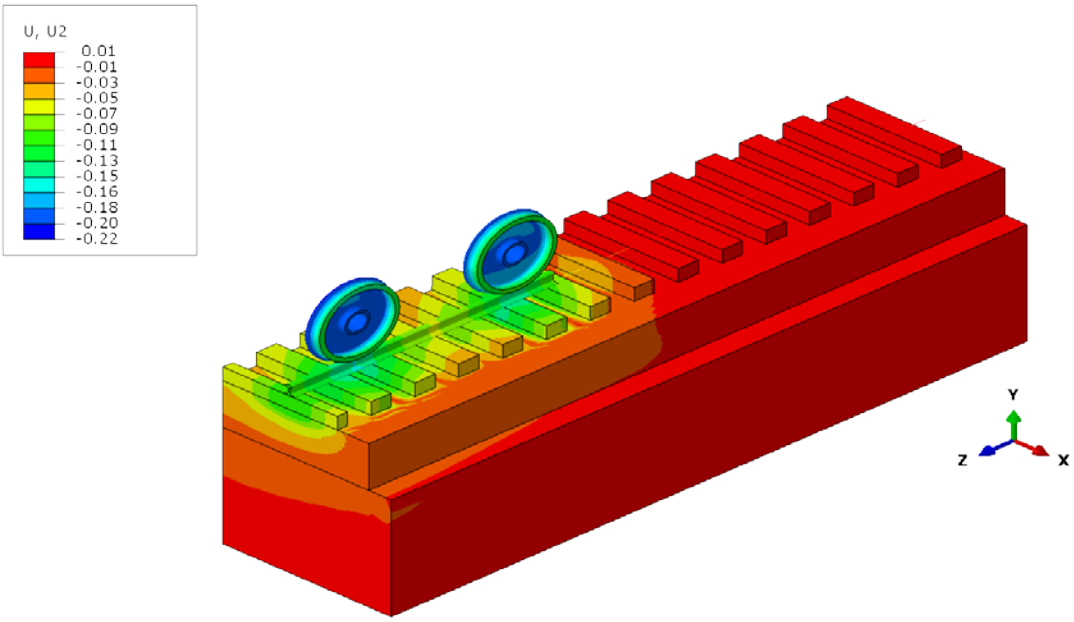

Figure 17. Vertical displacement (unit: inches) contour, the entire model, the case with worn rail profile and soft track support under higher wheel loads.

Figure 18. Vertical displacement (unit: inches) contour, the rail, the case with worn rail profile and soft track support under higher wheel loads, deformation magnified 30 times, structure mirrored with respect to the tank car center line.

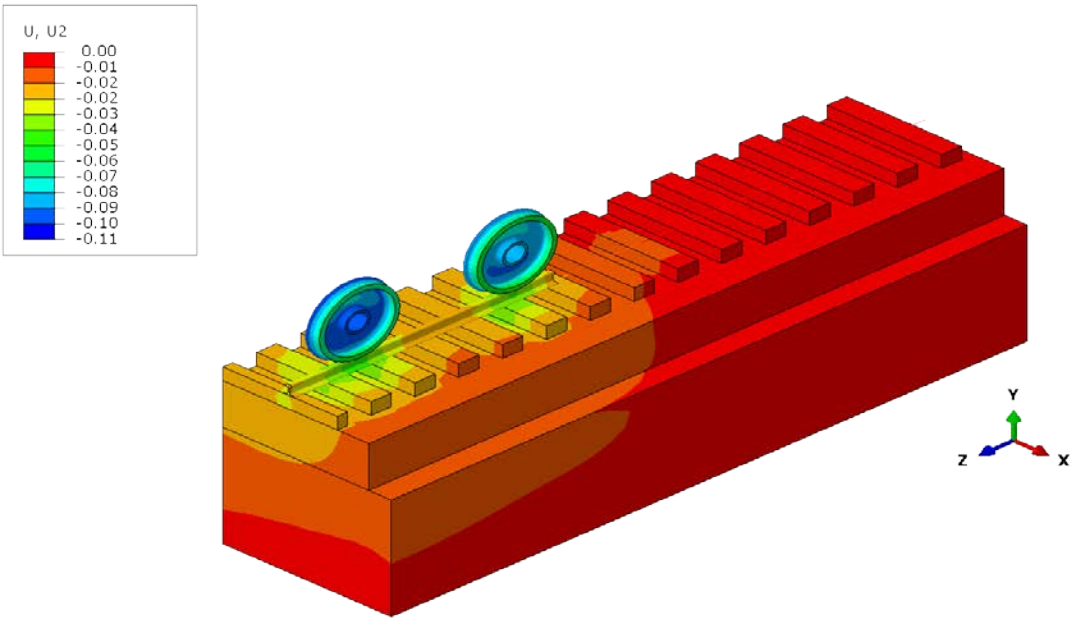

Figure 19. Vertical displacement (unit: inches) contour, the entire model, the case with standard rail profile and stiff track support under higher wheel loads.

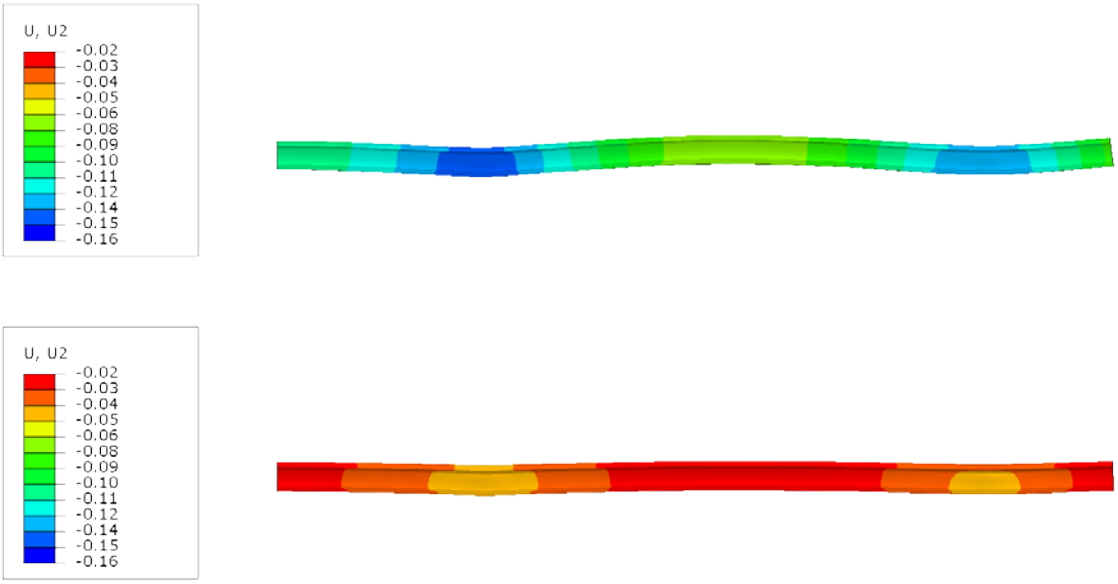

Figure 20. Comparison of the vertical displacement (unit: inches) contours on the rail between the two cases under higher wheel loads, deformation magnified 30 times: worn rail profile with soft track support (top) and standard rail profile with stiff track support (bottom).